<p style="text-align:center">カルシウムルーピングプロセスによる CO_2 と N_2O の同時排出低減</p>

Simultaneous reduction of CO₂ and N₂O emissions by Calcium-Looping Process

新潟大学工学部化学システム工学プログラム

教授　清水　忠明

Tadaaki Shimizu

Professor, Program of Chemistry and Chemical Engineering, Niigata University

Introduction

Calcium Looping (CaL) process, which uses CaO particles as sorbent, has been developed as a post-combustion CO_2 capture process as portrayed in Fig. 1[1]. In this process, dual-fluidized bed solid circulation system is usually employed. Carbon dioxide in flue gas from an air-blown combustor is captured by CaO in the carbonator at about 873 K. Decomposition of $CaCO_3$ to CaO and CO_2 is conducted in the regenerator at about 1223 K. The heat to decompose $CaCO_3$ in the regenerator is supplied by burning fuel such as coal with pure O_2 diluted by recirculated CO_2 so that the flue gas consists ideally only of CO_2 and H_2O. The CaL process is regarded as an energy-efficient and low-cost post-combustion CO_2 capture process[1-6]. Therefore, CaL process has been extensively investigated using mainly dual-fluidized bed systems to demonstrate CO_2 capture[7-20].
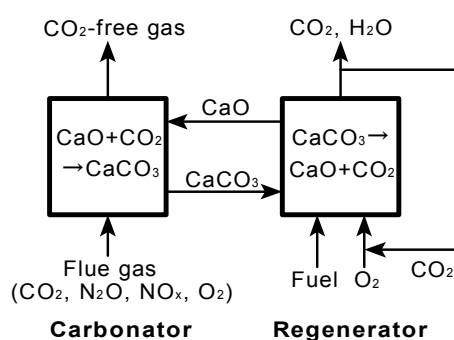

Fig. 1　Concept of CaL process

In addition to CO_2 capture, behavior of N_2O in the carbonator of CaL process is concern. N_2O is a greenhouse gas with high global warming potential (GWP) of 298[21]. Among air-blown coal combustors, circulating fluidized bed combustors (CFBCs) are known to release flue gas with relatively high N_2O concentrations of about 100–200 ppm (equivalent to 3–6% CO_2) during coal combustion[22-25]. Since the sorbent (CaO) particles are known to decompose N_2O at elevated temperatures[26-33], CaL process is expected to work as a process for N_2O decomposition as well as CO_2 capture, both of which contribute to the reduction of greenhouse gases.

The objective of this work is to clarify the reaction pathways of CO_2 and N_2O in the carbonator of CaL process. This work consists of three studies, 1)bubbling fluidized bed study to observe the fate of N_2O in the presence of CaO under

carbonator conditions, 2)dual-fluidized bed solid circulation system study to demonstrate N$_2$O decomposition and CO$_2$ capture, and 3)two-stage fluidized bed study to simulate solid circulation in the dual-fluidized bed solid circulation system. The last one, the two-stage system study, was designed to observe the behavior of N$_2$O decomposition and CO$_2$ capture under well-defined solid feed conditions; it is not easy to determine the solid circulation rate in the dual-fluidized bed system operated at high temperatures. Thus in the two-stage system study, a previously-calibrated screw feeder was employed to feed the sorbent at a desired feed rate.

Experimental

1. Bubbling fluidized bed experiments

Fig. 2 presents an illustration of a schematic diagram of a laboratory-scale bubbling fluidized bed system used for the present work. This fluidized bed was made of a quartz tube that had 26 mm inner diameter and total height of 1 m. A quartz sintered plate gas distributor was installed to support the solid sample. The solid sample was packed onto the distributor with a static bed height of 7 cm. The bed temperature was measured using a thermocouple (JIS Type-K). An electric heater heated the reactor to a fixed temperature of 873 K. A gas mixture of N$_2$O and O$_2$ diluted by N$_2$ was fed from the bottom. The superficial gas velocity was fixed at 17 cm/s at 873 K, i.e. the gas flow rate was 1.7 NL/min. The respective concentrations of N$_2$O and O$_2$ were fixed at 480ppm and 4%.

Calcined limestone was employed as the bed material. The composition (wt.%) of raw limestone included CaCO$_3$ 96.9, MgCO$_3$ 1.4, SiO$_2$ 0.6, Al$_2$O$_3$ 0.8, and Fe$_2$O$_3$ 0.3. The raw limestone particle size was 0.35–0.42 mm. The limestone was calcined in N$_2$ stream at 1173 K.
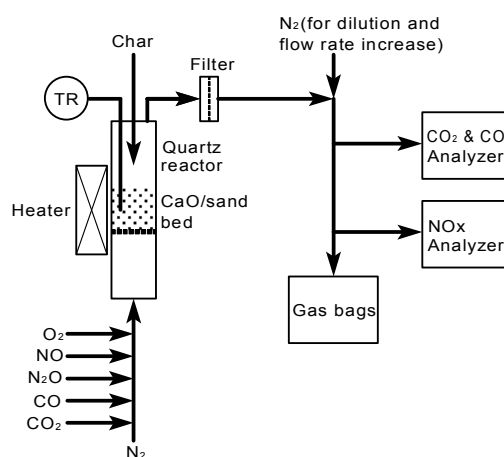

Fig. 2　Schematic diagram of a laboratory-scale bubbling fluidized bed system

2. Dual-fluidized bed experiments

Fig. 3 illustrates a schematic diagram of dual-fluidized bed system employed for the present work. This dual-fluidized bed system consisted of a bubbling fluidized

bed carbonator and a fast fluidized bed regenerator. The detail of the apparatus is given elsewhere[34)35)]. The carbonator was 9.3 cm in inner diameter and the bed height was fixed at 0.30 m by an overflow tube. The particles from the overflow tube were recirculated back to the bottom of the regenerator through a loopseal. The inner diameter and the height of the regenerator were 2.2 cm and 1.93 m, respectively. The particles were transported to the top of the regenerator by the upward gas stream, separated from the flue gas by a cyclone, and introduced into the carbonator. Gas mixture simulating flue gas from air-blown combustor consisted of CO_2, N_2O, O_2, and N_2 was fed to the carbonator. The concentration of CO_2 in the carbonator fluidizing gas was fixed at 15%. The concentration of N_2O was fixed at 240ppm. The O_2 concentration in the carbonator fluidizing gas was varied from 4% to 16.8%. The temperature in the carbonator was fixed at 873 K. The superficial gas velocity was 0.16 m/s at this temperature. The regenerator was fluidized by air without fuel feeding so that material balance of CO_2 could be evaluated. The superficial air velocity above the secondary gas inlet was fixed at 2.75 m/s (corrected at 1223 K). Gas leakage between two reactors was evaluated by feeding He and Ne as tracer gases to the regenerator and the carbonator, respectively. The gas leakage was found to be negligible.

The same limestone with different size from the bubbling fluidized bed experiments was employed as the bed material. The Sauter mean diameter of the raw limestone was 0.268 mm. The maximum size was 0.42 mm.
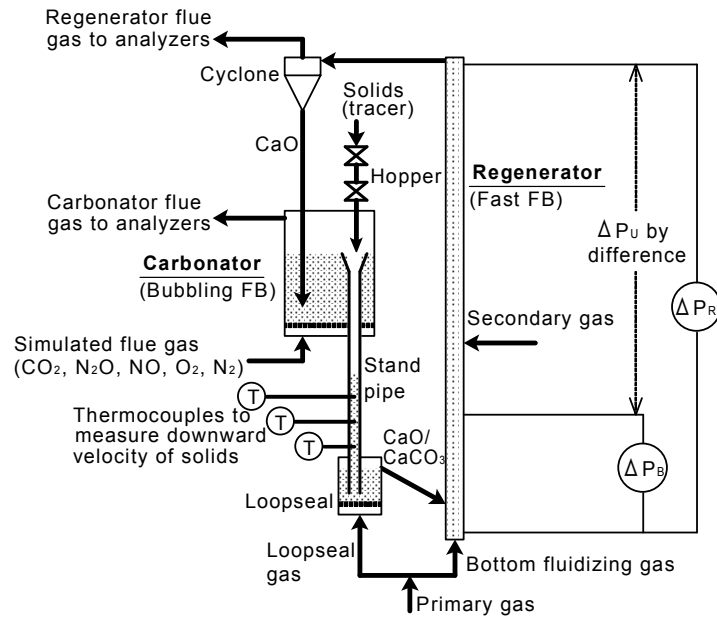

Fig. 3　Schematic diagram of dual-fluidized bed solid circulating system

3. Two-stage bubbling fluidized bed experiments

Fig. 4 illustrates a schematic diagram of two-stage fluidized bed system employed for the present work. This two-stage fluidized bed system consisted of two bubbling fluidized bed reactors of the same size connected in series. The inner

diameter and total height were 3.7 cm and 44 cm, respectively. An overflow tube was installed at 10 cm above the gas distributor. The first-stage fluidized bed reactor was used as a carbonator to which calcined limestone and simulated flue gas were fed. As the simulated flue gas, a mixture of CO_2, O_2, and N_2O diluted by N_2 was fed. The respective concentrations of N_2O and O_2 were fixed at 1000ppm and 4%. Superficial gas velocity was fixed at 0.10 m/s.

Calcined limestone particles were continuously fed from a hopper though a screw feeder to the top of the first-stage fluidized bed continuously. After partial carbonation, the solids withdrawn through an overflow tube of the first-stage fluidized bed was transported via a loopseal to the second-stage fluidized bed. The particles in loopseal were fluidized by N_2. The second-stage fluidized bed was used as a regenerator, into which nitrogen was fed as fluidizing gas to calcine $CaCO_3$. The calcined limestone particles withdrawn through an overflow tube of the second-stage fluidized bed was stored in a container purging the gas with inert gas (N_2). The solids stored in the container was then fed to the CaO hopper again, thus experiment was continued with solid sample using increased number of cycle. The condition of the regenerator was designed to establish the material balance of CO_2 capture in the carbonator and release of CO_2 in the regenerator, thus CO_2-free gas was fed to the regenerator.

For the calculation of the material balance, the split of fluidizing gas fed to the loopseal to the first stage and the second stage should be known. For the evaluation of the split, tracer gas (He) was fed to the loopseal fluidizing gas. The concentration of He in the gas samples was measured by gas chromatography. The tracer gas was detected in the gas samples from both the first-stage reactor and the second-stage reactor. This result indicates that the gas fed to the loopseal moved upward not only through the standpipe connecting the carbonator and loopseal but also the upward flow section of the loopseal connecting the regenerator and the loopseal. When the direct gas leakage occurred from the carbonator to the regenerator, He could not reach the carbonator. The fact that He was detected in the gas from carbonator indicated that upward flow of gas was formed in the downcomer of the loopseal.

The bed temperature was measured by use of thermocouples and controlled by use of electric heaters so that suitable temperatures for carbonation (873 K) and calcination (1223 K) were attained in the carbonator and the regenerator, respectively. The pressure drop between the bottom of the dense bed and the freeboard was measured to measure the solid hold-up in the reactors.

Calcined limestone sample after repeated use in the dual-fluidized bed system was employed. The solid sample was fed through a screw feeder to the top of the first-stage reactor. The relationship between the rotating speed of the screw and the feed rate of solids by bulk volume was calibrated in advance. Also the descending rate of the solid's surface in the hopper was measured intermittently, thus the bulk volume flow rate of the solids was calculated. By measuring the bulk density of the solids before packing into the solid hopper, the mass flow rate of the solids was estimated by multiplying bulk volume flow rate and the bulk density.
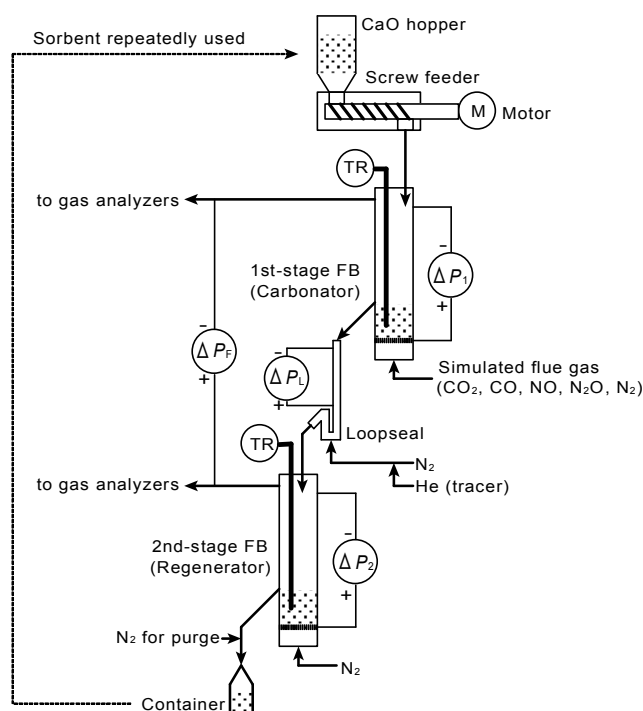
Fig. 4　Schematic diagram of two-stage fluidized bed system

The detail of the gas analysis is given elsewhere[21)22)]. The CO_2 and CO concentrations in the flue gas from the reactors were measured using NDIR absorption. Concentrations of NOx were continuously analyzed using chemical luminescence NOx analyzers. Flue gas samples were intermittently stored in gas bags. Concentrations of N_2O, He, and Ne in the gas samples were measured using gas chromatography with a thermal conductivity detector.

Results and Discussion
1. Bubbling fluidized bed experiments

The decomposition of N_2O was measured. When inert silica sand was employed as the bed material, the unreacted fraction of N_2O was about 98%, i.e., thermal decomposition of N_2O in the present fluidized bed apparatus was negligible. When CaO was employed, N_2O concentration in the produced gas was lower than the detection limit (2ppm), i.e. more than 99% of N_2O was decomposed in the CaO bed. This decomposition is attributable to the catalytic activity to decompose N_2O at elevated temperatures [26)-33)]. Thus calcined limestone can work as a catalyst for N_2O decomposition under a temperature condition of carbonator.

2. Dual-fluidized bed experiments

Fig. 5 shows a result of CO_2 capture in the carbonator and CO_2 release from the regenerator of dual-fluidized bed. Immediately after the start of CO_2 feed to the carbonator, the outlet flow rate of CO_2 from the carbonator decreased remarkably, *i.e.*, most of fed CO_2 was captured by CaO particles in the carbonator. With the

accumulation of captured CO_2 in the system, the rate of CO_2 release in the regenerator increased and finally the release rate of CO_2 reached the feed rate of CO_2 to the carbonator at about 1 hour after the start, *i.e.*, the material balance of CO_2 was closed.
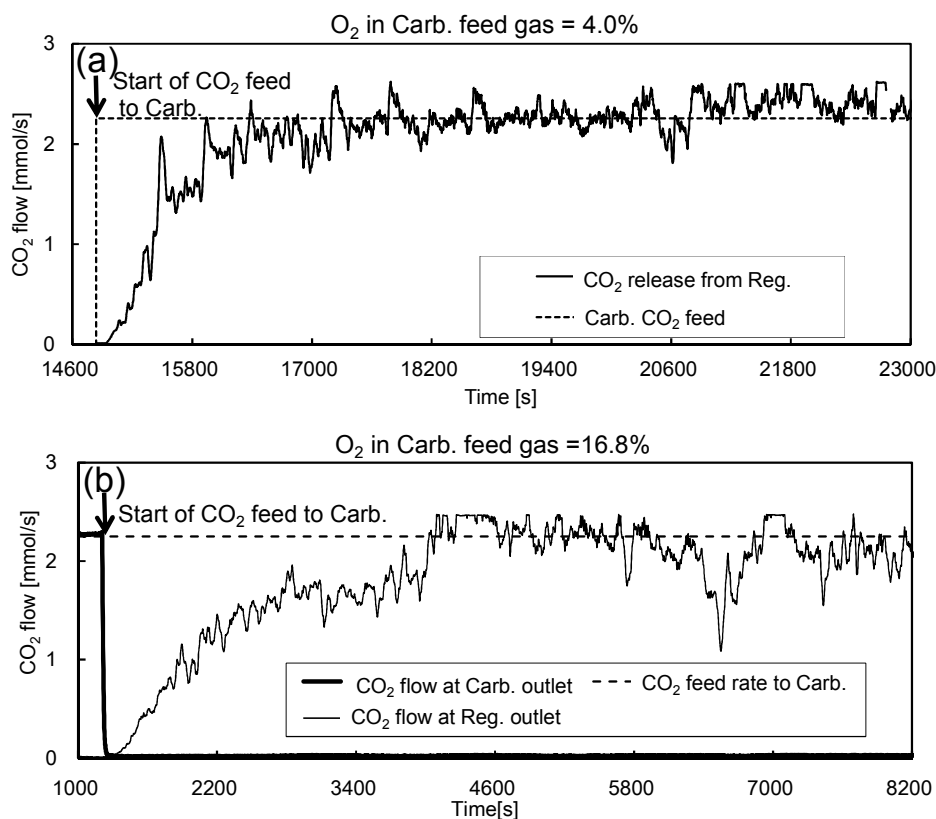

Fig. 5 CO_2 capture in carbonator and CO_2 release from regenerator of dual-fluidized bed

Fig. 6 shows the decomposition of N_2O in the carbonator of dual-fluidized bed. As expected from the results of bubbling bed experiments, the decomposition of N_2O was observed in the carbonator. Though the contact time (=solid volume/gas volume flow rate) of the carbonator of the dual-fluidized bed was longer than that of the bubbling bed apparatus, the conversion of N_2O observed for the carbonator of the dual-fluidized bed was lower than that of the bubbling fluidized bed. This is partly attributable to the decrease in solid activity after repeating carbonation/calcination cycles. For the bubbling bed experiments, fresh CaO particles after calcination of raw limestone were used, whereas the CaO particles used during dual-fluidized bed experiments had experienced a number of carbonation/calcination cycles. It is known that the CaO particles lose activity for CO_2 capture after repeating carbonation/calcination cycles because of sintering of grains[1) 36) 37)]. The reduced CO_2 capture capacity is attributable to the reduction of surface area through sintering of grains or plugging of small pores [38) 39) 40)]. Thus the activity to decompose N_2O is also considered to be reduced after repeating carbonation and calcination cycles.
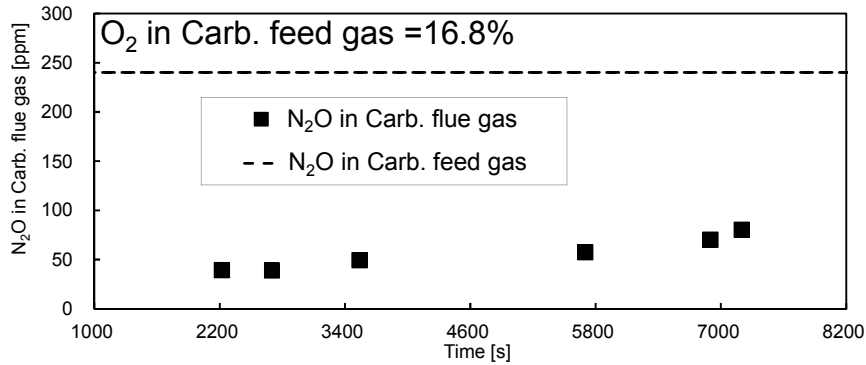
Fig. 6 Decomposition of N_2O in carbonator of dual-fluidized bed

3. Two-stage bubbling fluidized bed experiments

Fig. 7 shows the flow rates of CO_2 from the carbonator and the regenerator for different CaO feed rates. When CaO was fed, CO_2 was captured in the first-stage carbonator and the decomposition of $CaCO_3$ took place in the second-stage regenerator. Comparing the results obtained using the dual-fluidized bed system (Fig. 5), less CO_2 capture was observed. This difference is attributable to the lower bed height of the two-stage system (10 cm) compared with that in the dual-fluidized bed system (30 cm). For the analysis of the results, the present dual-fluidized bed system captured too much CO_2 to analyze the results; i.e. when the conversion of the reactant exceeds about 98%, the outlet concentration of the reactant is too low to determine the reaction rate from the ratio of the concentration at the inlet to that at the outlet. Thus conversion of the solid reactant was determined by the results of the two-stage fluidized bed system because both the inlet concentration and the outlet concentration could be determined with high accuracy.
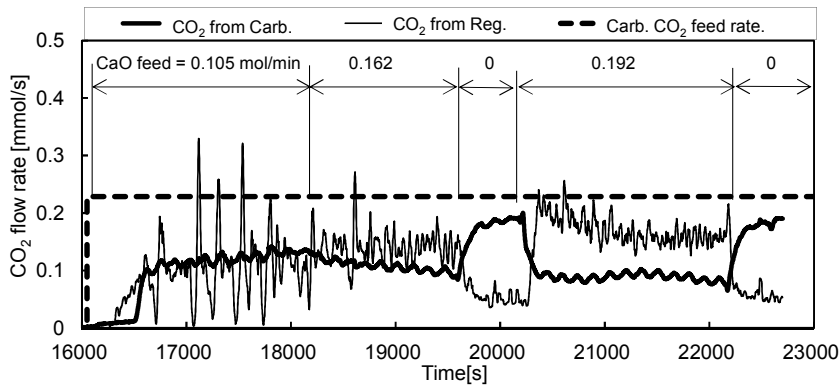

Fig. 7 Flow rate of CO_2 from carbonator and regenerator compared with CO_2 feed rate to carbonator observed using two-stage fluidized bed system

Fig. 8 shows the influence of CaO feed rate on CO_2 capture rate in the carbonator and conversion of CaO to $CaCO_3$ observed using two-stage fluidized bed system, where the conversion was calculated from the CaO feed rate and CO_2 capture rate. With increasing CaO feed rate, CO_2 capture rate in the carbonator increased, but
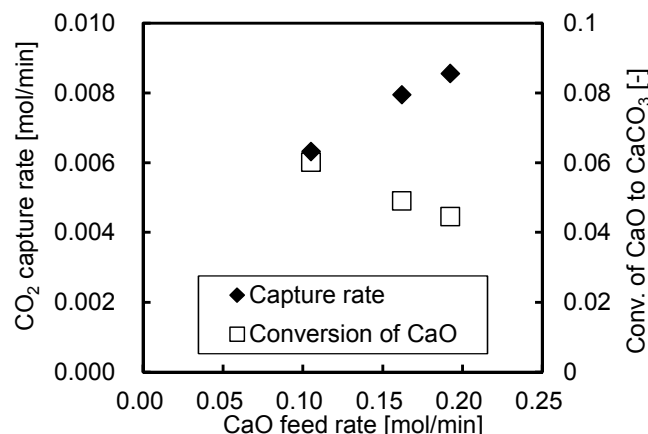
the conversion of CaO decreased.

Fig. 8　Influence of CaO feed rate on CO_2 capture rate in carbonator and conversion of CaO to $CaCO_3$ observed using two-stage fluidized bed system

Fig. 9 shows N_2O concentration normalized by N_2 concentration in the gas fed to carbonator and the flue gas from the carbonator. Because of the decrease in total gas flow rate after CO_2 capture, direct comparison of the concentration of N_2O in the fed gas with that at the outlet is meaningless, N_2 was employed for the inert tracer for the analysis of the conversion of N_2O. About 15% of fed N_2O was found to be decomposed in the carbonator. The decomposition of N_2O is attributable to the catalytic activity of CaO. The conversion of N_2O observed in the present two-stage fluidized bed system was lower than that of the present dual-fluidized bed system (Fig. 6). This difference is attributable to the difference in the bed height as discussed above.
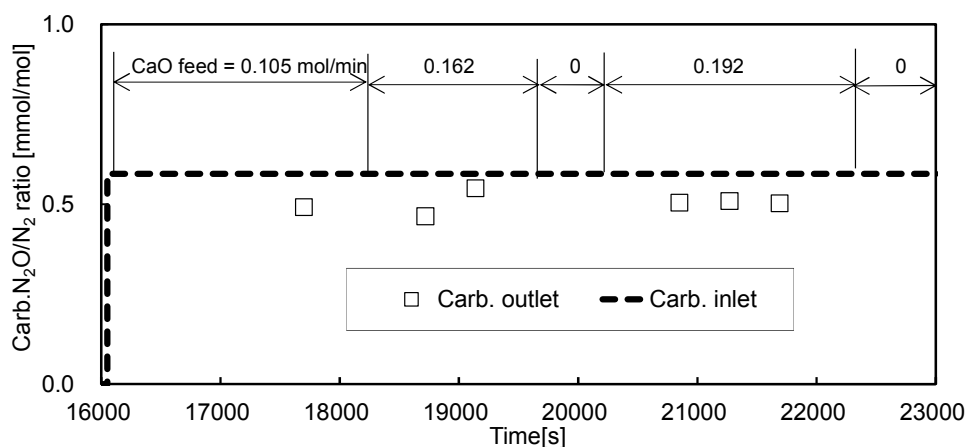

Fig. 9　N_2O decomposition in carbonator of two-stage fluidized bed system

Conclusion

The present work revealed that the sorbent of CaL process can work as a catalyst to decompose N_2O under a temperature condition of the carbonator of CaL process. Dual fluidized bed experiments revealed that a part of N_2O was

decomposed in the carbonator during continuous solid circulation with carbonation of CaO and calcination of produced $CaCO_3$. The two-stage fluidized bed experiments enabled the continuous model experiments of CaL process under precise solid feed conditions to obtain kinetic data of CO_2 capture and N_2O decomposition. CaL can be a multi-functional process for not only CO_2 separation but also for N_2O decomposition.

Acknowledgement

References

1) Shimizu, T.; Hirama, T.; Hosoda, H.; Kitano, K.; Inagaki, M.; Tejima, K., Chem. Eng. Res. Des., 77, 62–68 (1999)
2) Zhao, M.; Minett, A. I.; Harris, A. T., Energy Environ. Sci., 6, 25–40 (2013)
3) Atsonios, K.; Panopoulos, K.; Grammelis, P.; Kakaras, E., Int. J. Greenhouse Gas Control, 45, 106–117 (2016)
4) Hanak, D. P.; Biliyok, C.; Anthony, E. J.; Manovic, V., Int. J. Greenhouse Gas Control, 42, 226–236 (2015)
5) Clarens, F.; Espí, J. J.; Giraldi, M. R.; Rovira, M. ;Vega, L. F., Int. J. Greenhouse Gas Control, 46, 18–27 (2016)
6) Cormos, C. C., Appl. Therm. Eng., 82, 120-128 (2015)
7) Abanades, J.C.; Alonso, M.; Rodríguez, N.; González, B; Grasa ,G.; Murillo, R., Energy Procedia, 1, 1147–1154 (2009)
8) Alonso, M.; Rodríguez, N.; González, B.; Grasa, G.; Murillo, R.; Abanades, J. C., Int. J. Greenhouse Gas Control, 4, 167–173 (2010)
9) Arias, B.; Diego, M. E.; Abanades, J. C.; Lorenzo, M.; Diaz, L.; Martínez, D.; Alvarez, J.; Sánchez-Biezma, A., Int. J. Greenhouse Gas Control, 18, 237–245 (2013)
10) Charitos, A.; Hawthorne, C.; Bidwe, A.R.; Sivalingam, S.; Schuster, A.; Spliethoff, H.; Scheffknecht, G., Int. J. Greenhouse Gas Control, 4, 776–784 (2010)
11) Charitos, A.; Rodríguez, N.; Hawthorne, C.; Alonso, M.; Zieba, M.; Arias, B.; Kopanakis, G.; Scheffknecht, G.; Abanades, J. C., Ind. Eng. Chem. Res., 50, 9685–9695 (2011)
12) Dieter, H.; Hawthorne, C.; Zieba, M.; Scheffknecht, G., Energy Procedia, 37, 48-56 (2013)
13) Dieter, H.; Bidwe, A.R.; Varela-Duelli, G.; Charitos, A.; Hawthorne, C.; Scheffknecht, G., Fuel, 127, 23-37 (2014)
14) Fang, F.; Li, Z. S.; Cai, N. S., Ind. Eng. Chem. Res., 48, 11140–11147 (2009)
15) Kremer, J.; Galloy. A.; Ströhle, J.; Epple, B., Chem. Eng. Technol., 36, 1518–1524 (2013)
16) Lu, D. Y.; Hughes, R. W.; Anthony, E. J., Fuel Process. Technol., 89, 1386–1395

(2008)

17) Rodríguez, N.; Alonso, M.; Abanades, J. C., AIChE J., 57, 1356–1366 (2011)

18) Sánchez-Biezma, A.; Paniagua, J.; Diaz, L.; Lorenzo, M.; Alvarez, J.; Martínez, D.; Arias, B.; , Diego, M. E.; Abanades, J.C., Energy Procedia, 37, 1–8 (2013)

19) Ströhle, J.; Markus, J.; Kremer, J.; Galloy, A.; Epple, B., Fuel, 127, 13–22 (2014)

20) Symonds, R. T.; Champagne, S.; Ridha, F. N.; Lu, D.Y., Powder Technol., 290, 124–131 (2016)

21) IPCC, Fourth Assessment Report (AR4), Climate Change 2007: Working Group I: The Physical Science Basis, Chapter 2.10.2 Direct Global Warming Potentials, Table 2.14 (2007)
http://www.ipcc.ch/publications_and_data/ar4/wg1/en/ch2s2-10-2.html#table-2-14 (Last access 2015.2.7)

22) Åmand, L.-E., Leckner, B.; Dam-Johansen, K., Fuel, 72, 557 – 564 (1993)

23) de Diego, L. F.; Londono, C. A.; Wang, X. S.; Gibbs, B. M., Fuel, 75, 971 – 978 (1996)

24) Knöbig, T.; Werther, J.; Åmand, L.-E.; Leckner, B., Fuel, 77, 1635 – 1642 (1998)

25) Hiltunen, M.; Kilpinen, P., Hupa, M.; Lee, Y.-Y., Proc. 11th Int. Conf. on Fluidized Bed Combustion, 687-694, 21-24 April, 1991, Montreal, Canada

26) Iisa, K.; Salokoski, P.; Hupa, M., Proc. 11th Int. Conf. on Fluidized Bed Combustion, 1027-1034, 21-24 April, 1991, Montreal, Canada

27) Moritomi, H.; Suzuki,Y.; Kido, N.; Ogisu,Y., Proc. 11th Int. Conf. on Fluidized Bed Combustion, 1005-1012, 21-24 April, 1991, Montreal, Canada

28) Miettinen, H.; Stromberg, D.; Lindquist, O., Proc. 11th Int. Conf. on Fluidized Bed Combustion, 999-1004, 21-24 April, 1991, Montreal, Canada

29) Shimizu, T.; Tachiyama, Y.; Fujita, D.; Kumazawa, K.; Wakayama, O.; Ishizu, K.; Kobayashi, S.; Sikada, S.; Inagaki, M., Energy Fuels, 6, 753-757 (1992)

30) Shimizu, T.; Inagaki, M., Energy Fuels, 7, 648-654 (1993)

31) Shimizu, T.; Ishizu, K.; Kobayashi, S.; Shikada, H.; Inagaki, M., J. Jpn. Inst. Energy, 72, 189-198 (1993)

32) Johnsson, J. E.; Jensen, A.; Vaaben, R.; Dam-Johansen, K., Proc. 14th Int. Conf. on Fluidized Bed Combustion, 953-966, May 11-14, 1997, Vancouver, Canada

33) Shimizu, T.; Hasegawa, M.; Inagaki, M., Energy Fuels, 14, 104-111 (2000)

34) Gao, C.-Y.; Higuchi, T.; Yoshizawa, A.; Shimizu, T.; Kim, H.-J.; Li, L.-Y., Fuel, 121, 319–326 (2014)

35) Gao, C.-Y.; Takahashi, T.; Narisawa, H.; Yoshizawa, A.; Shimizu, T.; Kim, H.-J.; Li, L.-Y., Fuel, 127, 38–46 (2014)

36) Grasa, G.; Abanades, J. C., Ind.Eng. Chem. Res., 45, 8846-8851 (2006)

37) Abanades J.C.; Alvarez, D., Energy Fuels, 17, 308-315 (2003)

38) Abanades J.C.; Anthony, E.J.; Lu, D.Y.; Salvador, C.; Alvarez, D., AIChE J., 50, 1614-1622 (2004)

39) Sun, P.; Grace, J.R.; Lim, C.J.; Anthony, E.J., AIChE J., 53, 2432-2442 (2007)

40) Alvarez, D.; Abanades J.C., Ind. Eng. Chem. Res., 44, 5608-5615 (2005)